

CHAPTER FOUR

RESULTS AND DISCUSSION

4.1 Deformation Kinetics

This was characterized by two types of behavior when yield stress results at different temperatures and strain rates plotted in terms of $kT \log\left(\frac{\dot{\epsilon}}{\dot{\epsilon}_0}\right)$ against tensile yield stress as observed in Figure (4.1.1). The strain rates range from 10^{-1}s^{-1} to 10^{-7}s^{-1} with corresponding temperatures ranging from 17°C to 600°C . It is linear at the lower temperatures and high stresses but tends to curve at higher temperatures and lower stresses. This is possibly due to a change in deformation mechanism.

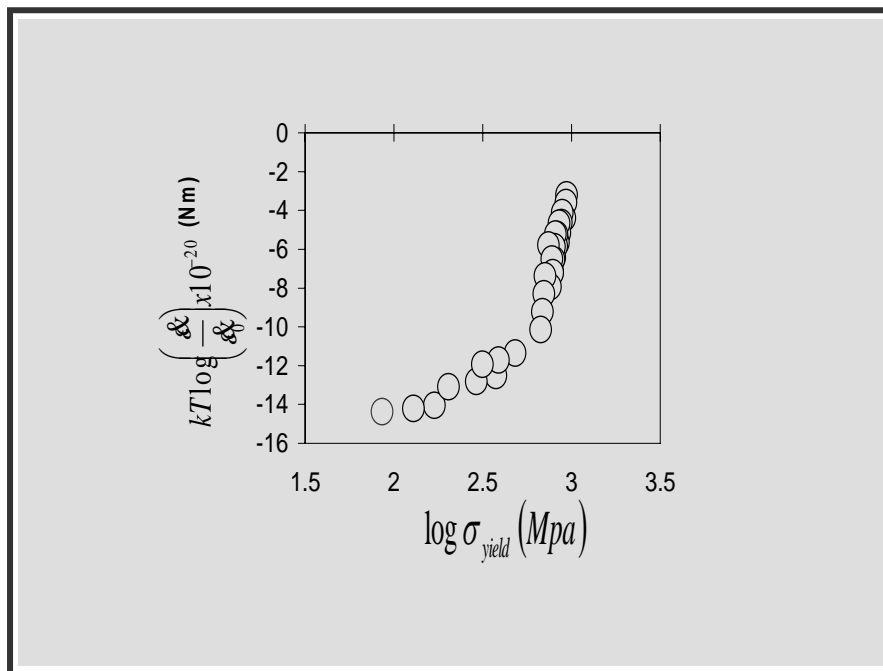


Figure 4.1.1: Strain rate versus yield stress at different temperatures and strain rates

Figure (4.1.2) below gives the linear part of the Figure (4.1.1). It can be seen that the points lay along a straight line as expected. The point of departure occurs at a stress level of 550Mpa. Below 550 MPa mechanism is probably due to glide of dislocation, whilst at stress level of above

550Mpa deformation mechanism can be attributed to climb of dislocation due mainly to power law / power law breakdown.

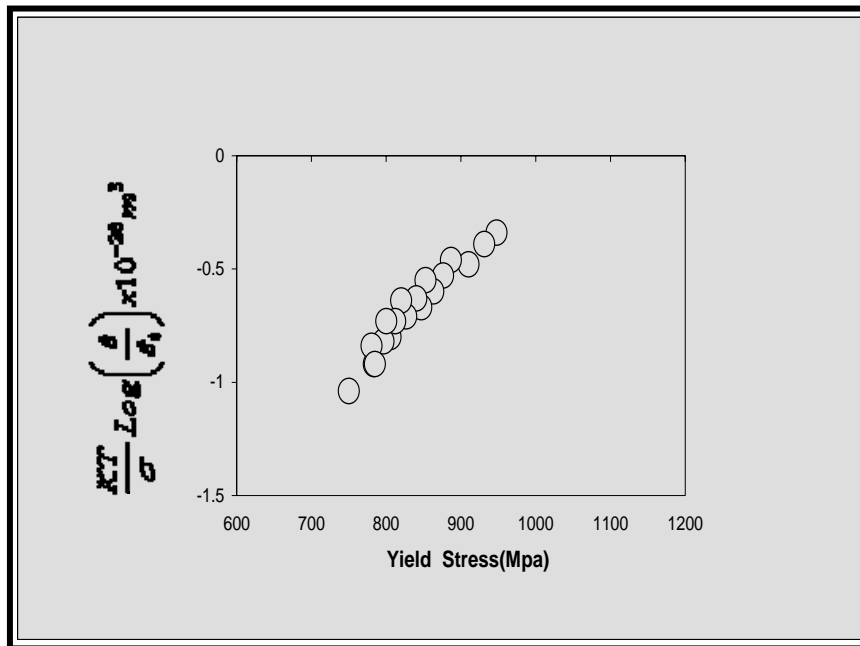


Figure 4.1.2: Strain rate plotted against tensile yield for specimen tested at strain rates and temperatures having yield stress above 550MPa.

The results for yield stress less than 550 MPa tend to lie on a curve which was generally derived from tests at higher temperatures (above about 500°C). For some metals at relatively high stresses and low temperatures, the rate controlling mechanism is often regarded as dislocation glide through an obstacle field, which may be provided by forest dislocations or precipitates.

When deformed at elevated temperatures, most metals and alloys obey a power creep law. However, as pointed out by Sherby et al⁹⁰ and Weertman⁹¹ at stress levels higher than about $5 \times 10^{-4} - 10^{-3} G$, where G is the shear modulus, the power law breaks down, and the creep rates are higher (and rise exponentially) than those predicted from an extrapolation from lower –stress (power law) regions. Sherby et al⁹⁰ suggested that the power-law breakdown might be associated with two contributing factors: (a) increased contribution from dislocation pipe diffusion and (b) excess vacancy generation. Ashby and Frost⁹²

suggested the power-law breakdown regime is a transition from diffusion-limited dislocation motion to the obstacle-limited glide regime. Arieli and Mukherjee⁹³ also indicated a similar approach, i.e., the power-law breakdown with increasing stress signifies a transition from diffusion controlled, dislocation climb related creep to glide controlled thermally activated dislocation mechanism. Raj and Langdon⁹⁴ came to a similar conclusion and suggested that high temperature climb is dominant in the power law creep region, while obstacle controlled glide occurring within the cell interiors is rate controlling in the power law breakdown region.

Along with the change in deformation mechanism, there is a change in the activation energy⁹⁵. Raj et al⁹⁶ observed that the deformed microstructure in metals in the primary creep region show a remarkable similarity with those formed in the exponential creep region. This observation is in accord with the conclusion that of Hammand et al⁹⁷ that, upon initial straining in creep, the substructure closely resemble those that are formed during strain hardening over the stage III deformation at lower temperatures, i.e., substructures related to thermally activated glide overcoming localised obstacles.

The fcc metals deform by dislocation interaction mechanism at low to intermediate temperatures and by creep to climb by edge dislocations at elevated temperatures. As mentioned earlier, the power law breakdown phenomenon was explained as a transition between dislocation climb and thermally activated glide. At constant stress, both mechanisms can operate simultaneously, but the mechanism that causes the highest strain rate will dominate over the certain range of temperatures. Arieli et al⁹³ assumed that the transition would occur during constant temperature creep tests at stress levels where the contribution of the two mechanisms to the strain rate is equal. Conversely, it can be said that at a constant applied strain rate, the transition occurs at that temperature where both mechanisms require the same stress to produce deformation rates equal to the applied strain rate.

4.2 Static Recovery Test

Recovery processes are those in which the structure and properties of a deformed and annealed metal partly revert to those of the undeformed material. The microstructural changes occurring during recovery mainly involve dislocations, and the grain structure is largely unaffected. The main processes occurring during recovery are the annihilation of dislocations of opposite sign and the rearrangement of remaining dislocations into configurations of lower energy as low angle boundaries. Recovery which occurs when the deformed metal is subsequently heated or annealed, it is known as static recovery. Recovery which occurs during hot deformation is known as dynamic recovery. Recovery typically starts around $0.3T_m$ (where T_m is the melting temperature in Kelvin) depending on the solute content.

Static recovery tests were carried out in this study by holding the specimens in the furnace for specific times and temperatures before carrying out tensile tests. The holding temperature ranging from 560°C to 640°C is high enough to facilitate recovery but low enough to prevent allotropic transformation with holding times ranging from one to 168 hours. When yield stress is plotted against holding times, asymptotic curves decaying towards the end were obtained. The curves tend to be more pronounced as the temperature and the holding time increase. This behavior is shown in figure (5.1.2) for total time limits of 0 and 2800×10^{-3} s and the strain rate of 1.5×10^{-4} 1/s.

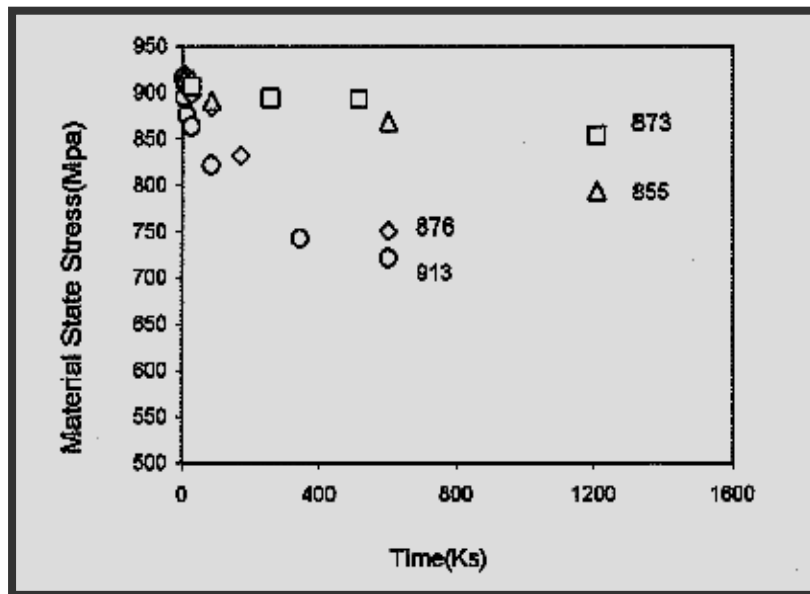


Figure 4.1.3: Behavior of material state stress for specimens aged at different times and temperatures.

Recovery in this type of material is generally attributed to dislocation annihilation/re-arrangement or particle coarsening or both. However, micro-analysis of a cross-section of some of the test specimen reveals little or no particle coarsening. Recovery could therefore be attributed mainly to dislocation rearrangement and annihilation. A similar study of such alloys reveals the same result³. There are three main processes whereby the excess stored energy due to dislocations may be released by recovery. First, the elimination of dipoles; secondly, the mutual annihilation of dislocations of opposite signs; and finally, the re-arrangement of the remaining dislocation into more stable arrays, processing lower values of strain energy (polygenisation). The first of these elementary recovery processes has been treated by Li⁹⁸ who has considered the annihilation of screw, edge and mixed dislocations dipoles. The behavior of edge dislocation dipole is more complicated than that of screw dislocation dipoles because of the existence of tangential forces between the edge dislocations.

To deal with all the dipoles in a deformed specimen a statistical treatment is necessary. By examining the existence of a set of non interacting dipoles, Li⁹⁸ shows that the kinetics for their annealing corresponds to a simple second order process. Subsequent to or concurrent with the disappearance of dislocation dipoles during annealing, the excess dislocations of one sign tend to rearrange into lower energy configurations. The simplest process of this kind is polygonisation which has been reviewed by Li⁹⁸.

Owing to the application of the electron microscope to the study of dislocation distribution in metals, it has now been recognized that polygonisation is a special form of sub-boundary formation. Most are formed even during deformation, as already mentioned, and these are called cell walls. During annealing, the dislocation distributions within the walls become more regular.

It is well known that low alloy steels have an unstable micro-structure and during prolonged periods at high temperatures, changes in precipitate type, size and spacing occurs. This results in change in the creep and fracture resistance of these alloys after long term exposure at high temperature.

4.3 Effect of Creep on Softening

The yield stress and by extension the hardness of materials that suffered creep before the tensile tests were conducted were correspondingly lower than the specimens that did not creep. The creep load was applied and the temperature was 79Mpa and 876K respectively in the tests carried out. As shown in figure (4.1.3a &b), the material tended to soften the longer the holding time for same the creep temperature and load.

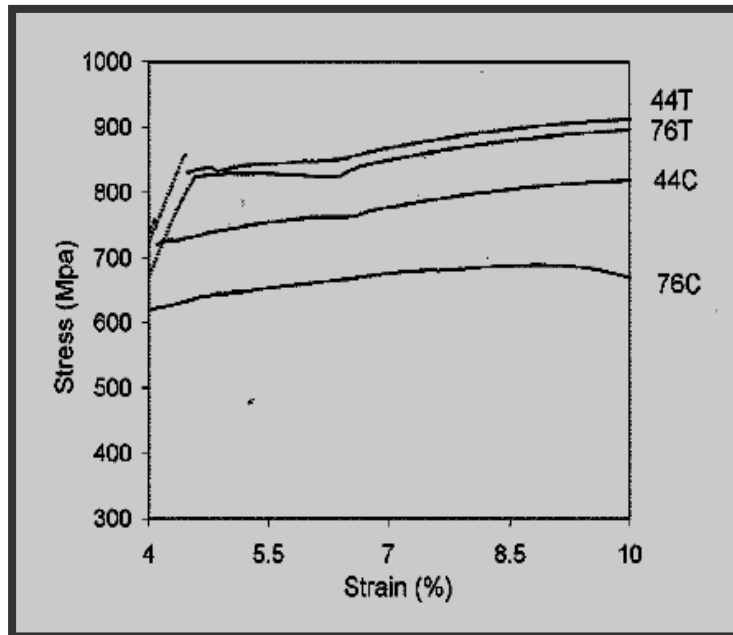


Figure 4.1.4a Experimental stress -strain curves for two sets of creep and tensile specimens.

Before carrying out the tensile tests, Specimens 44C and 76C underwent creep for 44 and 76 hours respectively while specimens 44T and 76T did not but were held with corresponding creep specimens for the corresponding times during the creep tests.

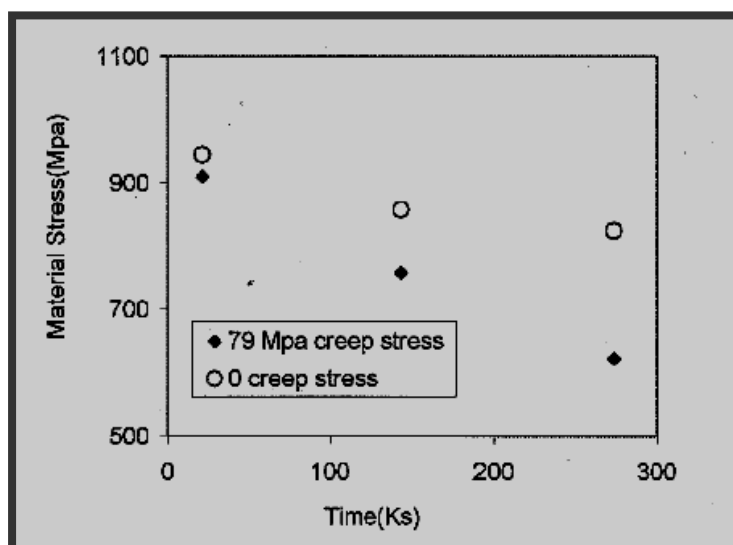


Figure 4.1.4b: Softening curves for specimens aged in the furnace and from interrupted creep tests.

It would be safe to conclude here that creep does indeed cause softening in the material under review. The recovery rate tends to be accelerated for material under stress (dynamic) compared to unstressed material (static)¹¹. During hot deformation of the metal, in addition to strain hardening caused by increase of dislocation density, the opposite phenomenon, i.e., strain softening caused by thermal activated processes can be observed. Softening can be attributed to recovery, recrystallization and strain localization. The load applied to the specimen that suffered creep facilitated dislocation arrangement and re-annihilation compared to the specimen that did not suffer creep for the same temperature.

4.4 Effect of Aging on Activation Energy

Stored energy of plastic deformation can be released by heating the metal to an elevated temperature. The metal softens due to release of stored internal energy.

The ageing process may involve a number of simultaneous processes (e.g., dislocation annihilation and re-arrangement, coarsening/dissolution of precipitates, formation of grain boundary precipitates, and the development of precipitate free zones). Typically, the models for these processes are not particularly well developed and attempts at summing up all of the relevant processes would probably result in very questionable results, making an empirical treatment more appealing.

In general, it would be prudent to consider effective activation energy for ageing, which would include all the on-going processes. In order to determine change in the activation energy with ageing, plots of yield stress at different temperatures versus $RT \ln\left(\frac{\dot{\epsilon}}{\dot{\epsilon}_0}\right)$ were used of specimens held in the furnace at 603°C for 24 and 48 hours respectively.

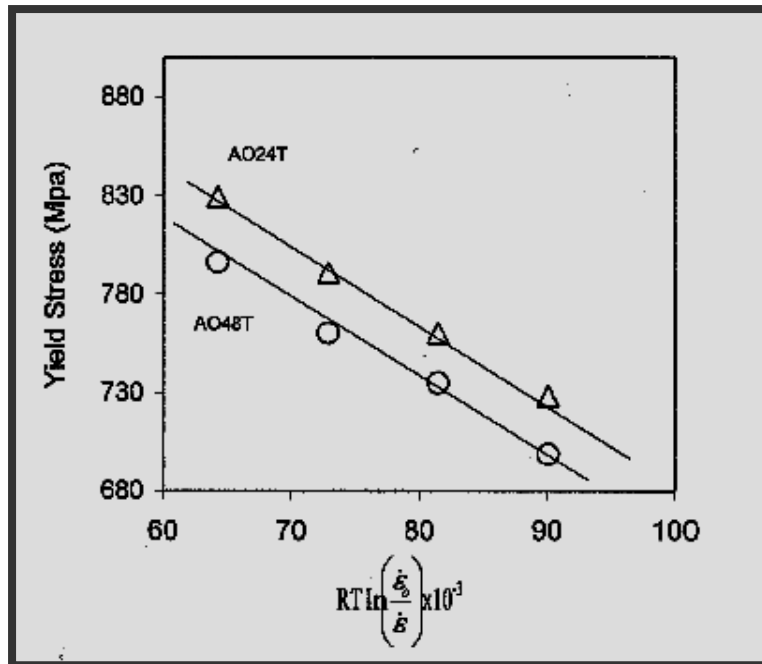


Figure 4.1.5: yield stress versus strain rates at different temperatures

The activation energy can be obtained from the gradient. The plot for the two ageing times is roughly parallel indicating equal gradients. Thus activation energy does not vary over a wide range for the ageing times used for the material.

4.5 Creep Curves

Experimental curves are compared for four different temperatures in figure (4.1.6--4.1.9). Strains are shown as true axial strains and stress values indicated were those at the beginning of each test. Since constant force testing was employed, stresses increased during creep and these increases were allowed for in the calculation, making the usual assumption that material volume is constant during plastic deformation. The curves illustrated have been truncated at strains corresponding to those at which specimens showed no visible signs of necking or void formation as evidenced by surface cracking. In general, specimens extended to fracture showed a further strain of order of 0.1 before failure, which was predominantly by necking with some cavitations near the fracture region.

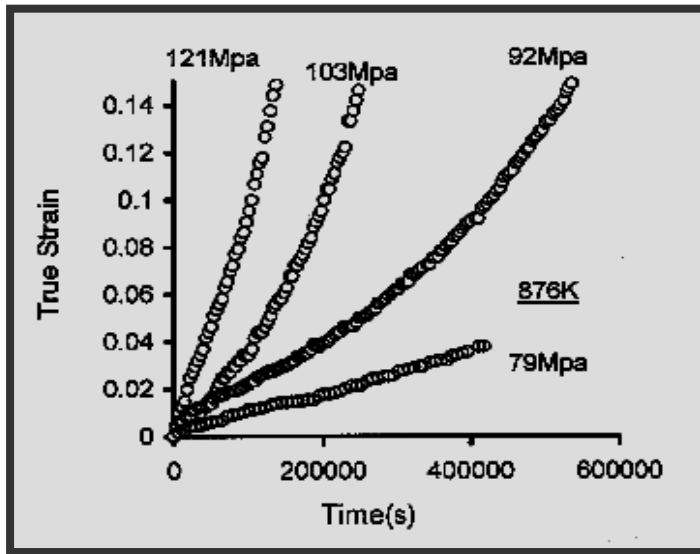


Figure 4.1.6.: creep results for a temperature of 564°C

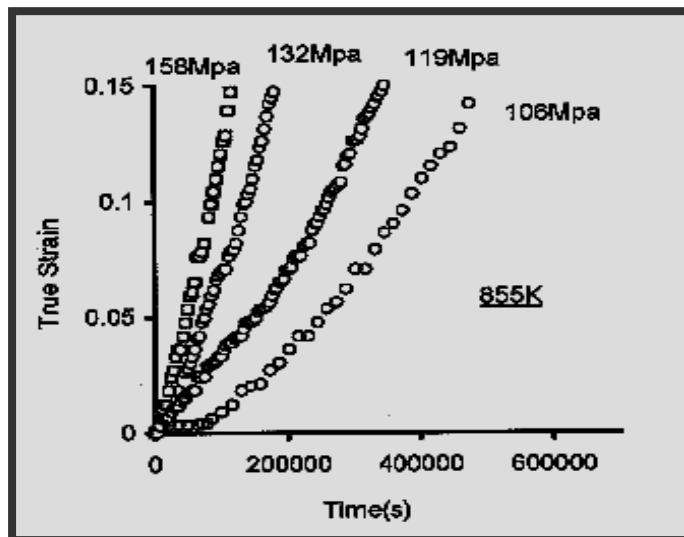


Figure.4.1.7: Creep results for a temperature of 582°C

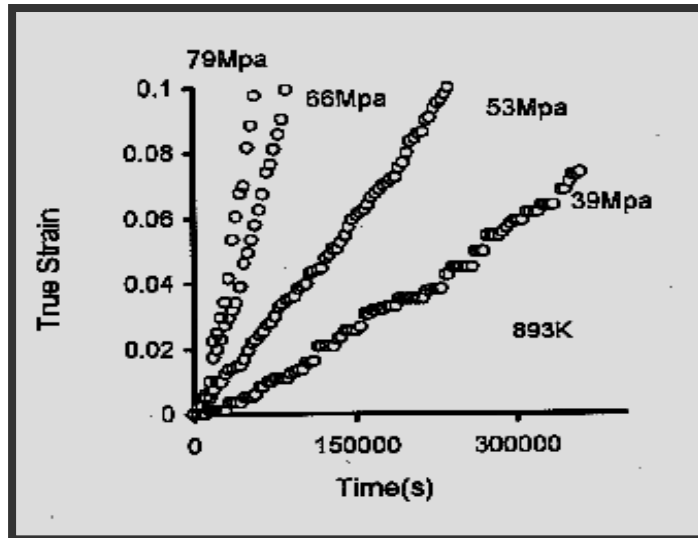


Figure 4.1.8: Creep results for a temperature of 603°C

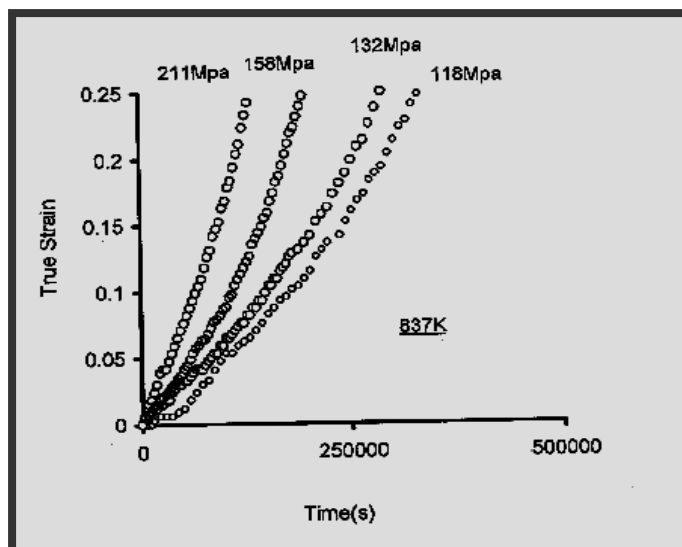


Figure 4.1.9: Creep results for a temperature of 620°C

The creep curves obtained for the alloy established that the relative extent of the primary stage diminished and the tertiary became more pronounced with decreasing stress and temperature. Furthermore, inspection of these curves demonstrates that it is artificial to define a "secondary" stage. Instead, with most metals and alloys, the decaying in creep rate during the primary stage is offset by the acceleration associated with damage processes, such as the development of grain

boundary cavities and / or the degradation processes, such as particle instability. Thus, the secondary creep rate is often a point of inflection, which can be ostensibly constant over a limited strain range. The only quantity which can be reasonably measured is the minimum creep rate. It is observed that the minimum creep rate occurs at a progressively early fraction of the life as the stress and temperature decreases.

As was expected, creep resistance of the material varied with both the stress and temperature. High stress and temperature favour high strain rate. High temperature and stress facilitate dislocation movement leading to re-arrangement and annihilation. At higher temperatures and lower stresses the rate controlling process becomes dislocation climb rather than glide. At intermediate stress and temperature, conditions between the glide (plasticity) and climb (power law creep) exist. This intermediate behaviour is known as power law breakdown. Power law breakdown is usually described by empirical equations or may be described by a combination of glide and power law equations.